Astronomy & Astrophysics manuscript no. Kagoshima
December 15, 2015
©ESO 2015

arXiv:1512.03892v1 [astro-ph.SR] 12 Dec 2015

Molecular jet emission and a spectroscopic survey of S235AB

R. A. Burns[1], T. Handa[1], T. Hirota[2,3], K. Motogi[4], I. Imai[1], and T. Omodaka[1]

[1] Graduate School of Science and Engineering, Kagoshima University, 1-21-35 Kôrimoto, Kagoshima 890-0065, Japan
e-mail: RossBurns88@Googlemail.com
[2] Mizusawa VLBI Observatory, National Astronomical Observatory of Japan, Osawa 2-21-1, Mitaka, Tokyo 181-8588, Japan
[3] Department of Astronomical Sciences, SOKENDAI (Graduate University for Advanced Studies), Osawa 2-21-1, Mitaka, Tokyo 181-8588, Japan
[4] Mizusawa VLBI Observatory, National Astronomical Observatory of Japan, 2-12 Hoshi-ga-oka, Mizusawa-ku, Oshu-shi, Iwate 023-0861, Japan

Received August 24, 2015; accepted December 12, 2015

ABSTRACT

Context. The S235AB star forming region houses a massive young stellar object which has recently been reported to exhibit possible evidence of jet rotation - an illusive yet crucial component of disk aided star formation theories.
Aims. To confirm the presence of a molecular counterpart to the jet and to further study the molecular environment in in S235AB.
Methods. We search for velocity wings in the line emission of thermal SiO (J=2-1, v=0), a tracer of shocked gas, which would indicate the presence of jet activity. Utilising other lines detected in our survey we use the relative intensities of intra species transitions, isotopes and hyperfine transitions to derive opacities, temperatures, column densities and abundances of various molecular species in S235AB.
Results. The SiO (J=2-1, v=0) emission exhibits velocity wing of up to 75 km s^{-1} above and below the velocity of the star, indicating the presence of a jet. The molecular environment describes an evolutionary stage resemblant of a hot molecular core.

Key words. Massive Star Formation – Jets – Stars; individual (S235AB)

1. Introduction

The target of our study, S235AB, is a star forming region that houses a massive young stellar object (MYSO) called S235AB-MIR - which was recently reported to exhibit fast ($\sim$ 50 km s^{-1}) jet-tracing water masers with a signature of rotation (Burns et al. 2015). The confirmation of a rotating jet in an MYSO would have great impact on theories of star formation as it would provide a method of removing angular momentum from the inner disk of the system - enabling accretion - while also corroborating a magneto-centrifugal launching mechanism for jets from massive young stars (*see* Konigl & Pudritz 2000).

S235AB-MIR is known to have slow molecular outflows (Felli et al. 2004), however, aside from the fast water maser velocities there is no evidence in the literature of a *fast* molecular jet in S235AB-MIR (Felli et al. 2004 claimed to have found a continuum jet aligned with the water maser jet, however they later retracted the claim in Felli et al. 2006). As a follow-up to the maser jet results of Burns et al. (2015) the primary aim of our spectral line survey was to find the molecular counterpart to the water maser jet in S235AB, which should be readily identifiable from doppler broadened line 'wings' seen in the thermal gas jet tracer SiO (J=2-1, v=0) (*for example* López-Sepulcre et al. 2011). The secondary aim of our observations was to further investigate the physical gas conditions in S235AB via basic astrochemical study using auxiliary spectral lines.

S235AB is known to have a dense molecular core centered on S235AB-MIR and molecular outflows mapped in HCO$^+$ (1-0) and C^{34}S (5-4) (Felli et al. 2004), CS (7-6) (Wu et al. 2010) and ^{13}CO (Felli et al. 1997). The *Spitzer* colours indicate that S235AB-MIR has a mass of 11 M$_\odot$, making it the only MYSO in the region (Dewangan & Anandarao 2011), and non-detection of centimeter emission in S235AB attests to its youth (Tofani et al. 1995; Felli et al. 2006).

2. Observations and Data Reduction

We conducted molecular line observations of S235AB in March and April of 2015 with the 45-m radio telescope of the Nobeyama Radio Observatory (NRO), a branch of the National Astronomical Observatory of Japan.

We observed in two sideband mode using the TZ receiver and we observed horizontal and vertical linear polarisations simultaneously. The upper sideband (USB) and lower sideband (LSB) central frequencies were 85.85 and 97.85 GHz, respectively, with band widths of 4 GHz each. The beamsize was about 18″. The SAM45 spectrometer provided 16 independent frequency arrays (8 per polarisation) which we organised to provide continuous coverage of a wide frequency range, and to include lines of particular interest. The frequency resolution was 244.14 kHz, providing a bandwidth of 1000 MHz per array.

Observing coordinates were centered to the position of S235AB-MIR at $(\alpha, \delta)_{J2000.0}$ = ($05^h40^m53^s.384$ +35°41'48".447). Sky-level subtraction was performed using a region of empty sky at coordinates $(\alpha, \delta)_{J2000.0}$ = ($05^h40^m58^s.30$ +35°41'48".60). Absolute flux calibration was performed using the chopper wheel method, empty sky and hot load. Pointing accuracy was checked using a nearby SiO maser source, RU Aur, every $\sim 1-2$ hours.

During the March observations the atmospheric conditions were good, with typical $T_{sys} \approx 140$ K, however strong wind conditions resulted in poor pointing accuracy and caused much of

Table 1. Summary of detected molecular lines and their measured parameters.

Molecular formula	Transition	T_A^* [K]	Obs Frequency [MHz]	Δv [MHz]	v_{peak} [km/s]	rms [K]
CH_3OH	2(1,2)-1(1,1) A++	0.230	95914.406	0.819	-17.22	0.012
$C^{34}S$	2-1	1.037	96413.016	0.852	-17.13	0.008
CH_3OH	2(-1,2)-1(-1,1) E	0.962	96739.445	0.778	-17.18	0.006
CH_3OH	2(0,2)-1(0,1) A++	1.330	96741.422	0.778	-17.14	0.012
CH_3OH	2(0,2)-1(0,1) E	0.461	96744.617	0.836	-17.21	0.016
CH_3OH	2(1,1)-1(1,0) E	0.210	96755.602	0.770	-17.29	0.007
$C^{33}S$	2-1 3/2-3/2	0.030	97169.438	0.811	-16.96	0.002
$C^{33}S$	2-1 1/2-1/2	0.151	97171.828	0.811	-16.96	0.002
$C^{33}S$	2-1 3/2-1/2	0.038	97175.188	1.155	-16.74	0.003
OCS	8-7	0.048	97301.203	0.786	-16.98	0.005
CH_3OH	2(1,1)-1(1,0) A–	0.191	97582.859	0.803	-17.16	0.005
^{34}SO	N,J=2,3-1,2	0.094	97715.461	0.868	-17.18	0.002
CS	2-1	3.639	97981.016	2.146	-17.19	0.019
CH_3CHO	5(1,4)-4(1,3) E	0.030	98863.484	1.262	-17.16	0.004
SO	N,J=2,3-1,2	1.531	99299.953	0.901	-17.14	0.013
CH_3OH	5(-1,5)-4(0,4) E	2.471	84521.188	3.170	-16.94	0.020
OCS	7-6	0.075	85139.250	0.606	-17.51	0.004
$HC^{18}O^+$	1-0	0.035	85162.375	0.959	-17.53	0.005
c-C_3H_2	2(1,2)-1(0,1)	0.093	85338.969	0.614	-17.22	0.005
HCS^+	2-1	0.129	85347.859	0.721	-16.96	0.004
CH_3CCH	5(2)-4(2)	0.034	85450.820	0.311	-17.19	0.004
CH_3CCH	5(1)-4(1)	0.058	85455.727	0.688	-17.22	0.003
CH_3CCH	5(0)-4(0)	0.085	85457.219	0.287	-16.72	0.001
$HC^{15}N$	1-0	0.157	86054.992	0.795	-17.09	0.005
SO	N,J=2,2-1,1	0.376	86093.984	0.721	-17.00	0.005
$H^{13}CN$	1-0 F=1-1	0.322	86338.750	0.786	-17.05	0.005
$H^{13}CN$	1-0 F=2-1	0.593	86340.180	0.811	-17.01	0.004
$H^{13}CN$	1-0 F=0-1	0.129	86342.242	0.688	-16.95	0.004
HCO	1(0,1)-0(0,0) 3/2-1/2 F=2-1	0.044	86670.648	0.664	-16.40	0.005
$H^{13}CO^+$	1-0	0.282	86754.352	0.746	-17.22	0.006
SiO	2-1 v=0	0.056	86847.023	1.901	-17.04	0.001
$HN^{13}C$	1-0 F=2-1	0.124	87090.812	0.705	-16.84	0.005
C_2H	1-0 3/2-1/2 F=1-1	0.137	87284.180	0.352	-17.08	0.003
C_2H	1-0 3/2-1/2 F=2-1	0.890	87316.969	0.770	-17.15	0.008
C_2H	1-0 3/2-1/2 F=1-0	0.479	87328.641	0.754	-17.06	0.006
C_2H	1-0 1/2-1/2 F=1-1	0.637	87402.102	0.778	-17.34	0.008
C_2H	1-0 1/2-1/2 F=0-1	0.296	87407.227	0.696	-17.21	0.010
C_2H	1-0 1/2-1/2 F=1-0	0.149	87446.523	0.819	-17.03	0.008

the on-source scans to suffer from beam warping and pointing offsets. Only 1 hour of observing session provided usable data.

During the April observations wind conditions were much better, providing good pointing accuracy (usually better than 3″), and T_{sys} was between 250 and 300 K. Data from the full 4 hour observing session was used.

To detect as many molecular lines as possible we interchanged between two frequency array setups which each covered different frequency ranges. The only frequency array common to both setups was that containing the SiO line - which was our transition of highest priority. Subsequently the frequency array containing the SiO line was observed for the full observing time while other frequency arrays were observed for roughly half of this time.

Data reduction was performed using the NEWSTAR software which was developed by the NRO. To reduce the aforementioned effect of the wind in the March observations we inspected all scans individually. Scans with bad pointing were determined by the failure in detecting $C^{34}S$, a rarefied gas whose region of peak emission is known to be compact from the maps of Felli et al. (2004) (their Figure 9). This greatly improved the quality of integrated spectra.

After flagging bad scans, 2^{nd} order polynomial baselines were fit to individual scans. Finally, all scans were integrated and polarisations were merged. Good scans on the target integrated to a total of 1 hour for the March data and 2 hours for the April data. The achieved sensitivity was typically better than 0.006 K for most frequency arrays, and reached 0.0025 K for the array containing the SiO emission. The antenna gain was roughly 4.4 Jy/K.

3. Results

Gaussian profiles were fit to spectral lines detected above 5 times the r.m.s noise. The detections and line parameters are listed in Table 1. Detected molecular transitions were identified by cross-referencing with the Cologne Database for Molecular Spectroscopy (CDMS) catalogue (Müller et al. 2005).

3.1. SiO - jet tracer

Our survey detected the common jet tracer transition line of SiO (2 – 1). In low temperature environments SiO molecules are confined to dust grains, resulting in a low gas abun-

dance. In a shocked gas environment these molecules are released from dust grains and become abundant in the gas phase (Martin-Pintado et al. 1992). As such SiO is a useful tracer of shocked gas and velocity wings in its spectrum indicate the presence of jets and outflows (López-Sepulcre et al. 2011). The spectrum of SiO (2 – 1) gas in S235AB is displayed in Figure 1, showing wide velocity wings.

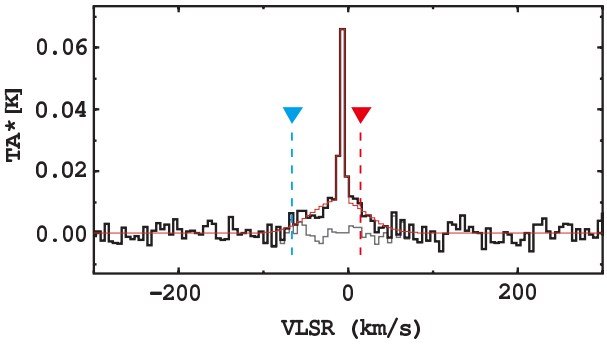

Fig. 1. Four channel binned spectrum of the SiO (2-1) emission in S235AB. Black lines show the observed data while the combined two Gaussian model and its residuals are shown in red and grey respectively. Blue and red triangles indicate extremum velocities of the H_2O masers of Burns et al. (2015).

3.2. Rotation Temperature

We detected multiple rotational transitions of Sulphur monoxide (SO) such that it was possible to estimate its rotation temperature, T_{rot}, by using the 'population diagram' method, detailed in Goldsmith & Langer (1999). Emission was optically thin and the derived rotation temperature was $T_{rot} = 26 \pm 4$ K which is similar to that obtained by Felli et al. (2004) of $\sim$ 30 K, using transitions of $CH_3CN(5-4)$.

We also measured the rotation temperature of methanol using transitions of CH_3OH (2-1), using lines of both E and A-species. The population diagram is shown in Figure 2, the slope giving $T_{rot} = 10 \pm 1$ K, and the gas optically thin. The line fit ignores the CH_3OH (5-4) E transition at $E_{upper} = 40$ K, which we discuss below. Methanol in this frequency regime is thought to be sub-thermally excited (Menten et al. 1988). Our estimate may therefore be considered as the lower limit of the kinematic temperature of the methanol cloud.

Multiple transitions of OCS were detected, but were too weak to attain a meaningful temperature estimate.

3.3. Detection of a class I methanol maser

The CH_3OH (5-4) E transition (84.521188 GHz) deviates from its expected excitation conditions as can be seen in the population diagram. This transition is known to exhibit maser behaviour (Menten et al. 1988), therefore it seems that we have detected maser emission at this transition in S235AB (Figure 3). The full line width of the emission is 11 km s^{-1} which is far too large to emanate from a single maser feature and thus indicates a likely blending of multiple features. The central velocity of this class I methanol maser is close to that of the molecular core, suggesting that it is not directly tracing the jet/outflow system and could instead be produced in the dense ambient gas somewhere near the outflow.

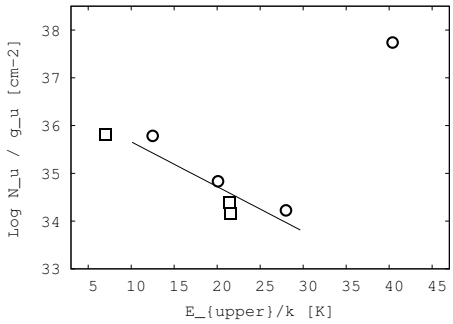

Fig. 2. Population diagram of CH_3OH in S235AB. E-and A-species are indicated by circles and squares respectively.

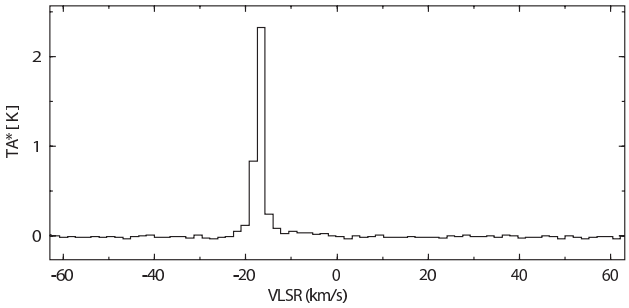

Fig. 3. Class I methanol maser emission spectrum from the CH_3OH (5-4) E transition at 84.521188 GHz.

3.4. Optical depth using hyperfine emission lines

Intensity ratios of the main line (F=2-1) to the hyperfine satellite line (F=1-0) of the C_2H molecule can be used to derive the gas optical depth via:

$$Line\ intensity\ ratio\ = \frac{1 - e^{-\tau}}{1 - e^{-a\tau}} \quad (1)$$

were a is the intrinsic line intensity ratio determined by laboratory experiment. For C_2H (F=1-0):(F=2-1), $a = 0.5$ in the optically thin limit (Tucker et al. 1974). Therefore, using Equation 1 our observed line intensity ratio of $T_A(1-0)/T_A(2-1) = 0.55$ gives $\tau_{C_2H} = 0.39$. This value is typical for young, massive star forming clumps (Sakai et al. 2010).

For optically thin $H^{13}CN$ the intrinsic intensity ratios of the hyperfine transitions (F=1-1):(F=2-1):(F=1-0) are 3:5:1 (Irvine & Schloerb 1984). Taking the transitions (F=2-1):(F=1-0)= 5, our observed intensity ratio of $T_A(F = 2-1)/T_A(F = 1-0) = 4.36$ gives $\tau_{H^{13}CN} = 0.07$.

3.5. Optical depth using isotopic abundance

We detected two isotopologues of two sulphur-bearing species; $C^{34}S$ and CS, and ^{34}SO and SO. We estimate the optical depths of CS and SO using the isotopologue line intensity ratios, as was done in Equation 1, where a is the intrinsic intensity ratio of $^{32}S/^{34}S = 22.5$ (Kahane et al. 1988). Our measured intensity ratio of $T_A(CS)/T_A(C^{34}S) = 4.9$ gives $\tau_{CS} = 5.1$, and our intensity ratio of $T_A(^{34}SO)/T_A(SO) = 15.2$ gives $\tau_{SO} = 0.9$.

3.6. Column densities and abundances

To estimate column densities from individual molecular species we used the prescription outlined in Goldsmith & Langer (1999) for species with measurable optical depths (*see* Sections 3.4 and 3.5) except for the column density of CH_3OH, which was obtained from the population diagram. For other molecules the statistical weights, upper energy levels, partition functions and Einstein coefficients for individual transitions were sourced from the Leiden Atomic and Molecular Database (LAMBDA) (Schöier et al. 2005) and CDMS catalogues with an assumed excitation temperature of 18.75 K with the exception for SO for which we used the measured rotation temperature (*see section 3.2*).

Saito et al. (2007) estimate the molecular hydrogen column density of the molecular core in S235AB to be 10.1×10^{22} cm^{-2} based on their $C^{18}O$ observations at comparable angular resolution. By comparing their results with the column densities measured in this work we estimated molecular abundances. These, alongside the aforementioned physical gas parameters, are summarised in Table 2.

Table 2. Summary of derived physical parameters.

Molecule	τ	T*rot* [K]	N_{Tot} [cm^{-2}]	Molecular abundance
C_2H	0.39	-	3.50E+15	3.5×10^{-8}
$H^{13}CN$	0.07	-	5.80E+13	5.7×10^{-10}
CS	5.1	-	6.63E+15	6.6×10^{-8}
SO	0.9	26 ± 4	9.76E+14	9.7×10^{-9}
CH_3OH	$\ll 1$	10 ± 1	7.85E+15	7.8×10^{-8}

4. Discussion and conclusions

Observations of S235AB by Sun et al. (2012) detected SiO emission at a peak brightness consistent with our observations however velocity wings were not detectable at the 0.017 K rms sensitivity of their observations. Our SiO spectrum (Figure 1) exhibits wide velocity wings reaching up to 75 km s^{-1} from the core velocity. Our deeper observations confirm the presence of a fast molecular jet in S235AB. Discovery of a high-velocity jet in this source is of particular significance in light of recent water maser results of Burns et al. (2015). Those authors find both blue-shifted and redshifted high velocity (~50 km s^{-1} from the core velocity) maser features in a bipolar configuration matching the alignment of the slow (< 5 km s^{-1} from the core velocity) NNW-SSE molecular outflow seen in HCO^+ and $C^{34}S$, reported by Felli et al. (2004).

The velocity of the SiO gas (~ 75 km s^{-1}) is much faster than that of the molecular outflow in S235AB making it likely that the SiO emission traces the primary molecular jet. Furthermore, as can be seen in Figure 1, the SiO jet gas and water masers have similar terminal velocities, suggesting likely association - although this should be confirmed with mapping observation.

Molecular outflows are thought to be produced as linear momentum from a protostellar jet is transferred into ambient gas around to the protostar. This gas becomes entrained at a slower velocity and at larger radii from the inner jet. The fast SiO gas in S235AB-MIR therefore indicates the presence of an entraining jet; the driving source for the water masers and molecular outflows seen in this region.

Burns et al. (2015) report evidence of possible jet rotation in their maser observations. Our confirmation of a molecular jet in S235AB-MIR introduce the possibility of investigating the spatial orientation of the jet via mapping observations - which may unearth further evidence of jet rotation.

Our survey investigated the physical properties of numerous molecular species in S235AB, which revealed a cold, dense gas environment with high opacity in several tracers - typical of the young cores in which MYSOs are embedded. Our survey results provide information on strengths and line widths of various gas tracers which will be useful for further follow-up observations.

We detected maser emission in the CH_3OH (5-4) E transition at 84.521188 GHz emanating from an ensemble of blended features. With regards to thermal CH_3OH emission at 97 GHz, we measured a low rotation temperature for the methanol gas, (~ 10 K), derived from the population diagram (Figure 3). In this respect S235AB conforms to the trend reported by Minier & Booth (2002) who find low rotation temperatures to be a systematic feature among their sample of massive star forming regions. They postulate that the 97 GHz methanol gas may trace cooler gas at the outer parts of the methanol cloud.

With regards to molecular abundances we compare our results to Gerner et al. (2014) who investigated a sample of 59 massive star forming regions categorised into different stages of evolution which, in order of ascending evolutionary stage are: infrared dark clouds, high mass protostellar objects, hot molecular cores and ultra compact H_{II} regions. A comparison with their results was possible for C_2H, SO, CS and CH_3OH which are common to ours and their works. For the cases of C_2H, SO, and CH_3OH our estimated abundances in S235AB are consistent with to the hot molecular core category of Gerner et al. (2014) (*see their* Figure 3), while CS matches somewhere between the hot molecular core and high mass protostellar object categories (*see their* Figure 5). The abundance of $H^{13}CN$ in S235AB is similar to those seen in another 5 well-studied massive star forming regions, the survey of which was reported in Zinchenko et al. (2009).

To conclude, the molecular abundances in S235AB are typical for a young massive star forming region. Its evolutionary stage close to that of a hot molecular core (*this work*, Felli et al. 2004) and preceding the formation of a HII region, as is indicated by the lack of centimeter emission (Tofani et al. 1995; Felli et al. 2006). Nonetheless it is a very active region as is evinced by the presence of slow molecular outflows (Felli et al. 2004), a maser jet (Burns et al. 2015), and a fast molecular jet.

5. Acknowledgements

We would like to thank staff at NRO for their generous support. We would also like to thank Takano Shuro for interesting discussion during the observing periods.

R.B. would like to acknowledge the Ministry of Education, Culture, Sports, Science and Technology (MEXT), Japan for financial support under the Monbukagakusho scholarship.

T. Hirota is supported by the MEXT/JSPS KAKENHI Grant Numbers 24684011, 25108005, and 15H03646

H.I. is also supported by the JSPS KAKENHI Grant Number 25610043.

K.M. is supported by a Grant-in-Aid from the JSPS Fellows and JSPS KAKENHI Grant numbers 24-6525 and 15K17613.

References

Burns, R. A., Imai, H., Handa, T., et al. 2015, MNRAS, 453, 3163
Dewangan, L. K. & Anandarao, B. G. 2011, MNRAS, 414, 1526
Felli, M., Massi, F., Navarrini, A., et al. 2004, A&A, 420, 553

Felli, M., Massi, F., Robberto, M., & Cesaroni, R. 2006, A&A, 453, 911
Felli, M., Testi, L., Valdettaro, R., & Wang, J.-J. 1997, A&A, 320, 594
Gerner, T., Beuther, H., Semenov, D., et al. 2014, A&A, 563, A97
Goldsmith, P. F. & Langer, W. D. 1999, ApJ, 517, 209
Irvine, W. M. & Schloerb, F. P. 1984, ApJ, 282, 516
Kahane, C., Gomez-Gonzalez, J., Cernicharo, J., & Guelin, M. 1988, A&A, 190, 167
Konigl, A. & Pudritz, R. E. 2000, Protostars and Planets IV, 759
López-Sepulcre, A., Walmsley, C. M., Cesaroni, R., et al. 2011, A&A, 526, L2
Martin-Pintado, J., Bachiller, R., & Fuente, A. 1992, A&A, 254, 315
Menten, K. M., Walmsley, C. M., Henkel, C., & Wilson, T. L. 1988, A&A, 198, 253
Minier, V. & Booth, R. S. 2002, A&A, 387, 179
Müller, H. S., Schlöder, F., Stutzki, J., & Winnewisser, G. 2005, Journal of Molecular Structure, 742, 215
Saito, H., Saito, M., Sunada, K., & Yonekura, Y. 2007, ApJ, 659, 459
Sakai, T., Sakai, N., Hirota, T., & Yamamoto, S. 2010, ApJ, 714, 1658
Schöier, F. L., van der Tak, F. F. S., van Dishoeck, E. F., & Black, J. H. 2005, A&A, 432, 369
Sun, Y., Xu, Y., & Yang, J. 2012, CAA, 36, 238
Tofani, G., Felli, M., Taylor, G. B., & Hunter, T. R. 1995, A&AS, 112, 299
Tucker, K. D., Kutner, M. L., & Thaddeus, P. 1974, ApJ, 193, L115
Wu, J., Evans, II, N. J., Shirley, Y. L., & Knez, C. 2010, ApJS, 188, 313
Zinchenko, I., Caselli, P., & Pirogov, L. 2009, MNRAS, 395, 2234